PAPER

Luminescent, bimetallic AuAg alloy quantum clusters in protein templates†

Jyoti Sarita Mohanty,[a] **P. Lourdu Xavier,**[a] **Kamalesh Chaudhari,**[ab] **M. S. Bootharaju,**[a] **N. Goswami,**[c] **S. K. Pal**[c] **and T. Pradeep**[*a]

We report the synthesis of luminescent AuAg alloy quantum clusters (QCs) in bovine serum albumin (BSA), for the first time, with experimentally determined atomic composition. Mixing of the as-synthesized protein-protected Au and Ag clusters resulted in the formation of alloy AuAg clusters within the BSA. Mass spectrometric analysis of the product of a 1 : 1 molar ratio reaction mixture of Au_{QC}@BSA and Ag_{QC}@BSA suggested that the alloy clusters could be $Au_{38-x}Ag_x$@BSA. Further analyses by standard techniques revealed that the alloy cluster core of ~1.2 nm diameter is composed of nearly zero valent Au and Ag atoms that exhibit distinctly different steady state and time resolved excited state luminescence profiles compared to the parent clusters. Tuning of the alloy composition was achieved by varying the molar ratio of the parent species in the reaction mixture and compositional changes were observed by mass spectrometry. In another approach, mixing of Au^{3+} ions with the as-synthesized Ag_{QC}@BSA also resulted in the formation of alloy clusters through galvanic exchange reactions. We believe that alloy clusters with the combined properties of the constituents in versatile protein templates would have potential applications in the future. The work presents interesting aspects of the reactivity of the protein-protected clusters.

1. Introduction

Atomically precise molecules of noble metals with quantum confined phenomena have been some of the most fascinating materials in molecular cluster science in the recent past.[1–6] They are groups of atoms with a sub–nanometer sized core, considered to be the missing link between atoms and nanoparticles, and we refer to them as quantum clusters (QCs). Intense luminescence, unusual photo-stability, novel catalytic properties and several other phenomena have caused excitement in this branch of science. Because of the sp → sp intraband and sp → d interband transitions occurring in them, they are luminescent and their luminescence can be tuned by controlling the number of atoms in the core. Clusters of Au and Ag have been among the most studied clusters in the solution phase.[1–4] Several methods in the solution phase,[1] as well as in the solid state,[7] have been used to synthesize metallic clusters. From the characterization point of view, among the different techniques, mass spectrometry has

been an indispensable analytical tool to understand the atomic composition of metallic clusters.[6] The possibility of manipulating their properties through precise variations in composition has prompted the exploration of alloy clusters. Recently, monolayer-protected alloy clusters like $AuAg_{144}$ and $AuAg_{38}$, Pd-doped Au clusters and AuAg alloy clusters stabilized by chitosan in the solid state have been demonstrated.[8–11] A recent example of manipulation in alloy composition is the creation of a stable 13-atom AuAg alloy of such clusters by our group.[12] The most recent category of these new materials is their analogues in protein templates such as Au_{25}@BSA, Au_{38}@BSA, $Au_{13,25}$@NLf, Ag_{15}@BSA and Au_{16}@BSA.[13–17] The bright emission of clusters in protein and peptide templates has been exploited for bio-labelling.[3,14,18] Various bio-medically important functional proteins such as lactotransferrin[15] and insulin[21] have been used to synthesize such clusters and the latter is shown to retain bioactivity.[3,19,20] Hence, these new analogues hold huge potential in the bio-medical field. While intense luminescence, bio-compatibility and facile targeting capability have been demonstrated with these systems, structural properties and the precise compositional manipulation of the cluster core are still being explored.[3,22,23] The creation of such a cluster goes through multiple steps involving metal ion uptake in an intermediate valance state and its subsequent reduction involving concomitant inter-protein metal transfer.[23] While various questions concerning the growth, structural and optoelectronic properties of clusters in protein templates have yet to be answered, their intense luminescence has resulted in several applications. In this

[a] *DST Unit of Nanoscience, Department of Chemistry, Indian Institute of Technology Madras, Chennai-600 036, India. E-mail: pradeep@iitm.ac.in*
[b] *Department of Biotechnology, Indian Institute of Technology Madras, Chennai-600036, India*
[c] *Unit for Nanoscience and Technology, Department of Chemical, Biological and Macromolecular Sciences, Satyendra Nath Bose National Centre for Basic Sciences, Block JD, Sector III, Salt Lake, Kolkata 700 098, India*

† Electronic supplementary information (ESI) available: XPS, SEM EDAX, UV-Vis, PL and FTIR measurements. See DOI: 10.1039/c2nr30729d

paper, we explore the precise compositional manipulation of cluster cores leading to AuAg alloys across the entire compositional window. This becomes feasible in the AuAg alloy system as they form solid solutions in the entire compositional range. The results propose that stoichiometric reactions are possible in the case of clusters within proteins, which suggests a dynamic interaction between the cluster core and the medium. Such compositional changes occur on fast timescales, implying chemistry analogous to molecular systems. The cluster core is susceptible to galvanic chemistry leading to etching.[12] This supports the existence of cluster nuclei within them with larger electrochemical potential compared to the parent bulk metal, allowing facile electron transfer to isolated ions. Applications of alloy cluster systems in electronics, catalysis and in medicine have enormous potential. The longer lifetime possessed by these non-photobleachable luminescent clusters becomes an attractive option in fluorescence life-time imaging.[4]

2. Experimental

2.1. Reagents and materials

Tetrachloroauric acid trihydrate ($HAuCl_4 \cdot 3H_2O$) was purchased from CDH, India. Silver nitrate ($AgNO_3$) and sodium hydroxide (NaOH) were purchased from Rankem, India. BSA was purchased from the Sisco Research Laboratory. Sodium borohydride ($NaBH_4$) was purchased from Spectrochem, India. Sinapinic acid was used as the matrix for matrix assisted laser desorption ionization mass spectrometry (MALDI MS). All chemicals were used as received without further purification.

2.2. Instrumentation

UV-Vis spectra were collected using a PerkinElmer Lambda 25 instrument in the range of 200–1100 nm. Luminescence measurements were carried out on a Jobin Yvon NanoLog instrument. The band pass for excitation and emission was set as 3 nm. Picosecond-resolved fluorescence decay transients were measured by using a commercially available spectrophotometer (Life Spec-ps, Edinburgh Instruments, UK) with 60 ps instrument response function (IRF). The observed fluorescence transients were fitted by using a nonlinear least squares fitting procedure to a function $(X(t) = \int_0^t E(t')R(t - t')dt')$ comprising of the convolution of the IRF $(E(t))$ with an exponential sum$(R(t) = A + \sum_{i=1}^{N} B_i e^{-t/\tau_i})$ with pre-exponential factors (B_i), characteristic lifetimes (τ_i) and a background (A). The relative concentration in a multi-exponential decay was finally expressed as: $c_n = \frac{B_n}{\sum_{i=1}^{N} B_i} \times 100$. The quality of the curve fitting was evaluated by a reduced χ-squared analysis and residual data. It should be noted that with our time resolved instrument, we can resolve at least one quarter of the instrument response time constants after the de-convolution of the IRF. X-Ray photoelectron spectroscopy (XPS) studies were conducted with an Omicron ESCA probe spectrometer with polychromatic Mg K_α X-rays (hv = 1253.6 eV). The samples were spotted as drop-cast films on a sample stub. A constant analyser energy of 20 eV was used for the measurements. MALDI MS studies were conducted using a Voyager DE PRO Biospectrometry Workstation from

Applied Biosystems. A pulsed nitrogen laser of 337 nm was used for the MALDI MS studies. Mass spectra were collected in linear positive mode and were averaged for 100 shots. Scanning electron microscopy (SEM) and energy dispersive analysis of the X-ray (EDAX) images were collected using an FEI QUANTA-200 SEM. For the SEM and EDAX measurements, samples were spotted on an indium tin oxide (ITO) conducting glass substrate and dried in ambient conditions. High resolution transmission electron microscopy (HRTEM) was performed with a JEOL 3010, 300 kV instrument equipped with an ultra high resolution (UHR) pole piece. Samples were prepared by dropping the dispersion on carbon coated copper grids for HRTEM. Solid-state FTIR spectra were measured with a PerkinElmer instrument. KBr crystals were used as the matrix for preparing the samples. Far-UV circular dichroism (CD) spectra were measured with a Jasco 815 spectropolarimeter.

2.3. Alpha-helix calculation

The alpha helix content from the obtained CD spectra was calculated by the formula proposed by Chen et al.[24] α-helix (%) = $-(\theta + 3000)/39\,000$, where $\theta = MRW \times \theta_{222}/10lc$, where MRW is mean residual weight, l is path length of the cell and c is the concentration of the sample used for the measurement. The MRW of BSA is 114, the concentration of the protein used for the measurements was 2×10^{-7} g mL^{-1} and the path length of the cell used was 1 cm.
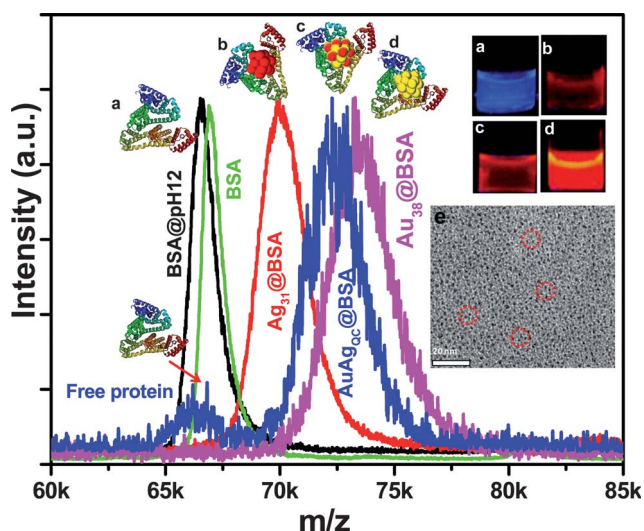
2.4. Synthesis

Au and Ag QCs were synthesized in protein templates as reported previously.[12,16] Briefly, Au_{QC}@BSA was synthesized by mixing solutions of BSA and $HAuCl_4$ to get final concentrations of 169.0 µM and 4.4 mM, respectively (the molar ratio of the protein to Au^{3+} was 1 : 26), along with the addition of 100.0 µL 1.0 M NaOH to make the final volume 1.1 mL. Then the mixture was stirred vigorously for 8 h until the solution turned golden brown in colour. Similarly, Ag_{QC}@BSA was also synthesized by mixing the protein and $AgNO_3$ solutions to get a final concentration of 169.0 µM and 4.4.0 mM, respectively (1 : 26 molar ratio) and 100.0 µL of 1.0 M NaOH was added to make the final volume ~1.1 mL. 1.0 µL of 0.05 M freshly prepared $NaBH_4$ was added to the reaction mixture and stirred for ten minutes until the solution turned golden brown. Note that here the final molarities of Au^{3+} and Ag^+ used for the individual Au and Ag cluster synthesis were kept the same in order to carry out further alloy cluster synthesis reactions. The as-synthesized Au_{QC}@BSA and Ag_{QC}@BSA were mixed together and stirred for 4 h to form alloy clusters in different v/v ratios. In a second approach, to the as-synthesized Ag_{QC}@BSA, different volumes (10, 25, 50 and 80 µL) of 100 mM $HAuCl_4$ were added to make a different final concentration of Au^{3+} in the reaction mixture and stirred vigorously for 8 h. All the samples were directly taken from the reaction product for the MALDI MS and for time dependent measurements, samples were collected at appropriate time intervals.

3. Results and discussion

3.1. Formation of the alloy cluster through QC–QC interaction

Isolated gold and silver clusters protected with proteins, especially BSA, have been characterised in detail.[3,13,16] At specific molar ratios of metal ions to proteins, they produce well defined clusters exhibiting sharp peaks in the MALDI MS spectra. These mass shifts from the parent protein give the size of the metal cluster nucleus and it also implies the presence of a specific cluster within a single protein.[12,23] We chose to make Ag and Au clusters (Ag_{QC}@BSA and Au_{QC}@BSA) with ∼31 and ∼38 atoms, respectively in the core, although other cluster nuclei are possible by incubating varying concentrations of the metal ions. Fig. 1 is the comparison of the MS spectra of the Au, Ag and AuAg alloy clusters formed in BSA. The formation of the alloy clusters ($AuAg_{QC}$@BSA) can be inferred from the occurrence of a mass spectral feature in between the parent Au and Ag clusters with the simultaneous absence of both the parent clusters. Along with these, there is an emergence of the BSA feature confirming the appearance of the free protein[23] (Fig. 1). The alloy formation leads to a distinct change in photoluminescence, as seen from the inset photographs in Fig. 1a–d. It may be noted that MALDI MS is quantitative and can be used to determine the relative concentration of species, however, the peak intensities do not reflect the true concentrations of the species in the sample due to differences in their ionization efficiencies.

The calculated mass difference between the monocation peak of QC@protein and intact protein suggests the number of atoms in the cluster core. BSA in NaOH has a peak at m/z 66 500, which is shifted by 300 to lower m/z when compared to the protein at neutral pH (m/z 66 800). This can be attributed to the concomitant modifications occurring due to the breakage of disulfide

bonds or deamidation at extreme pH. Au_{QC}@BSA has a peak at m/z ∼73 900 and Ag_{QC}@BSA has a peak at m/z 69 900. The calculated mass difference between Au_{QC}@BSA and BSA is ∼7.5 kDa, indicating the formation of Au_{38} (Fig. 1). The possibility of the formation of Au_{38}@BSA has already been reported by our group.[14] The difference between Ag_{QC}@BSA and BSA was ∼3.4 kDa, suggesting the formation of ∼Ag_{31}. Finally, the difference between $AuAg_{QC}$@BSA and the protein was ∼5.9 kDa, suggesting the formation of $(AuAg)_{38}$. Since the atomic ratio (in Au and Ag) used was 1 : 1, the composition could be Au_{19} : Ag_{19}. Since a definite understanding of the mechanism of cluster–cluster interaction is not yet available, several other possibilities of composition may also be possible. It is almost impossible to determine the exact mass from the mass spectra due to the inherent uncertainty at this high mass. The possibility of the formation of $(AuAg)_{38}$ nanomolecules in the case of monolayer-protected clusters has been demonstrated recently.[9] It is likely that such a system could also be synthesized in protein templates. It is important to note that the parent cluster peaks do not exist in the reaction product; however, the peak corresponding to the free protein appears and this has been probed further (see below).

HRTEM analysis showed that the cluster cores are ∼1.2 nm in size (Fig. 1 inset). TEM is not an appropriate tool, unlike MS, to investigate the clusters, since electron beam induced growth of the clusters[25] would give an exaggerated cluster size. However, it is useful to know the approximate size and rule out the possibility of the presence of bigger plasmonic nanoparticles. Here, it is clear that the emission shown in the inset photographs of Fig. 1 comes from non-plasmonic particles. It is important to confirm that plasmonic particles are not formed in solution due to cluster–cluster interactions.

Alloy clusters of one specific composition (($AuAg)_{38}$ obtained by mixing clusters at a 1 : 1 molar ratio) were investigated in detail to understand the variation in their properties in comparison to the parent clusters. These studies revealed systematic changes in the cluster properties. For example, the absorption spectra are almost the same in all the cases and no distinct features were observable, unlike in the case of monolayer-protected clusters[8–10,12,13] (Fig. 2A). However, broad peaks of poor intensity in between 300 and 600 nm were observed in the case of the Ag clusters. Au_{38}@BSA did not show any absorption peak, as in the case of other protein-protected gold clusters,[13,14,23] and the lack of prominent absorbance features in such systems is under investigation. In the case of the alloy, although broad peaks from Ag_{QC}@BSA were faintly visible initially, the spectrum became featureless with time. This change in the optical spectra could be due to the alloy cluster formation, as suggested by the MALDI MS. As no spectral features of the parent clusters were seen in the MALDI MS after the reaction, the new peak is attributed to the alloy. Here we have to note that the reason for the absence of distinct optical peaks in such clusters, quite unlike monolayer-protected clusters, is still under investigation. The presence of such peaks would have allowed the cluster core size to be deciphered. The luminescence emission maximum of the alloy cluster shifts to red (∼707 nm) at this composition compared to the Au (∼660 nm) and Ag (∼670 nm) clusters (Fig. 2B) when excited at 370 nm. Multiple excitation peaks were observed as expected for QCs in proteins due to the cluster core
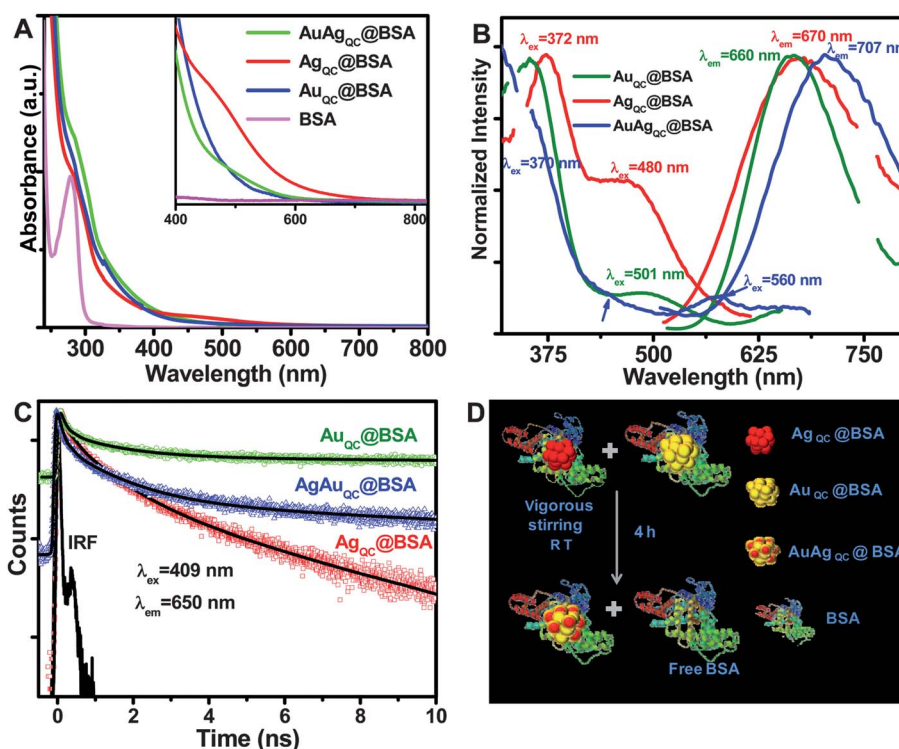

Fig. 1 MALDI MS data showing the formation of the alloy cluster. Positive ion mass spectra of BSA (green solid line), BSA at pH 12 stirred for 12 h (solid black line), Au_{QC}@BSA (solid magenta line), Ag_{QC}@BSA (solid red line) and $AuAg_{QC}$@BSA (solid blue line). Cartoons above the mass spectra show the different clusters formed. Insets: photographs under UV-light of (a) BSA, (b) Ag_{QC}@BSA, (c) $AuAg_{QC}$@BSA and (d) Au_{QC}@BSA. (e) TEM image of $AuAg_{QC}$@BSA shows a core size of ∼1.2 nm. The scale bar in the TEM image is 20 nm.

Fig. 2 (A) UV–Vis spectra of BSA, Au$_{QC}$, Ag$_{QC}$, and AuAg$_{QC}$@BSA. (B) PL spectra of Au$_{QC}$ (green line), Ag$_{QC}$ (red line), and AuAg$_{QC}$ (blue line) @BSA. Emission spectra were collected for all the three clusters by exciting them at 370 nm. (C) Picosecond-resolved fluorescence transients of Au$_{QC}$ (green), Ag$_{QC}$ (red), AuAg$_{QC}$ (blue) @BSA. (D) Schematic of the synthesis of AuAg@BSA alloy clusters through QC–QC interaction.

as well as the protein.[23] Au$_{QC}$@BSA has two excitation maxima at ~370 and 504 nm and Ag$_{QC}$@BSA has excitation peaks at ~370 and 480 nm, as previously reported.[14–16] AuAg$_{QC}$@BSA showed excitation peaks at ~370, 470 and 560 nm. Time resolved measurements revealed tri-exponential decay for all the clusters and gave the following lifetime values: Ag$_{31}$@BSA – 0.16 ns (55%), 0.96 ns (33%) and 3.9 ns (12%); Au$_{38}$@BSA – 0.14 ns (64%), 1.30 ns (24%) and 32.9 ns (12%); (AuAg)$_{38}$ – 0.12 ns (71%), 1.20 ns (22%) and 11.8 ns (7%) (Fig. 2C and Table 1). From the above data, it is evident that the lifetime of the alloy cluster is distinctly different from its parent clusters. It should be mentioned that we have tried to fit the decay profile of the alloy clusters to different combinations of the lifetimes of the Au and Ag QCs, however, none of these combinations fitted well, revealing the presence of a new emitting species. The calculated quantum yield values for Au$_{QC}$@BSA, Ag$_{QC}$@BSA and AuAg$_{QC}$@BSA were 6.8, 1.9 and 2.8%, respectively, with rhodamine 6G as the reference.

Immediately upon addition of Au$_{QC}$@BSA to Ag$_{QC}$@BSA, both the parent cluster peaks vanished and a new peak at m/z ~72 600 appeared, implying a fast QC–QC interaction (Fig. 3).

Table 1 Lifetime components of the parent Au, Ag and alloy clusters in the protein template. The numbers in the parentheses indicate relative weights (standard error 10%)

| QC system	τ_1 (ns)	τ_2 (ns)	τ_3 (ns)	τ_{av} (ns)
Ag$_{31}$@BSA	0.16 (55%)	0.96 (33%)	3.9 (12%)	0.51
Au$_{38}$@BSA	0.14 (64%)	1.30 (24%)	32.9 (12%)	3.40
(AuAg)$_{38}$@BSA	0.12 (71%)	1.20 (22%)	11.8 (7%)	0.85

Although the chemical interaction between the clusters is fast, there are distinct time dependent changes, as expected for such large molecular systems. The time evolution of the MALDI MS spectra over the course of one day revealed the gradual emergence of the free BSA peak, along with the alloy nucleation. Until the second hour of incubation, the peak remained at the same position and from the fourth hour of incubation, the mass increased and the peak was around m/z 73 600, coinciding with the emergence of the free protein. This increase in mass is attributed to the incorporation of metal ions released from the parent clusters in the initial stages of the reaction. Slow reduction and metal incorporation is seen in such systems.[23] The alloy clusters are not as stable as their parent analogues. As Fig. 3 shows a similar position for the parent protein, it is clear that cluster-containing proteins do exchange metal ions between them, and concomitantly free protein emerges. Protein based synthesis procedures involve highly dynamic structural changes in the protein's secondary structure as a function of time to facilitate the cluster synthesis. Here, we have to note that amino acid metal ion interaction is also dynamic.[23,26] These data imply a chemical substitution reaction retaining a similar number of core atoms, as metal atom transfer from the protein during cluster incubation is feasible.[23] Similar processes may be facile in fully grown clusters as well. The wrapping of a single metal cluster non-covalently, with multiple thiol groups anchored on the cluster surface by a single large organic molecule, is possible where the flexible conformations are feasible.[27] Similarly, it is likely that a high molecular weight protein with a large number of thiols could completely wrap metallic clusters with multiple-thiol anchoring points. Dynamic light scattering (DLS) studies
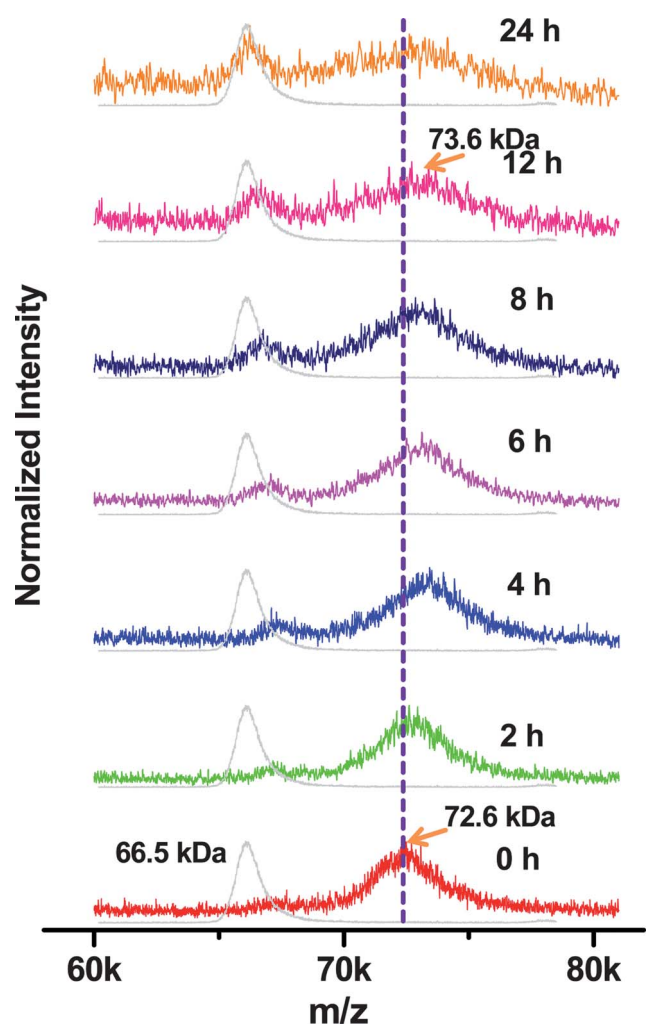
Fig. 3 Time-dependent MALDI MS data of AuAg$_{QC}$@BSA show the emergence of the free protein and also the shifting of the cluster-containing protein peak from m/z 72 600 (0 h) towards m/z 73 600 (12 h) as a function of time.

have shown the absence of any aggregate other than a slightly larger sized protein, supporting the presence of a cluster within.[13,19]

The existence of the alloy is confirmed using elemental analysis by SEM-EDAX and XPS. In the specific case of a 1 : 1 alloy, EDAX confirms the composition of the alloy cluster to be 1 : 1 in Au : Ag (Fig. S1†). The presence of the alloy cluster has been further strengthened by the observations made in the XPS analysis, which indicated the presence of a metallic core and hence rules out the possibility that the presence of complexes to be the reason for the observed MS pattern and the cause of the emission. In XPS, the Au 4f and Ag 3d regions support the zero-valent state for both the elements (Inset of Fig. 4). The Au 4f$_{7/2}$ and Ag 3d$_{5/2}$ peaks appear at 84.1 and 368.2 eV, respectively, close to the metallic values. These are the same positions seen in metal clusters protected with monolayers and proteins.[12–16] The S 2p$_{3/2}$ and 2p$_{1/2}$ peaks occurred at 162.1 and 163.3 eV, respectively (Fig. S2†), which are the characteristic features of thiolate.[28] Thus, it is evident that the cluster core is stabilized by the thiol groups of the protein (predominantly from the cysteine residues,
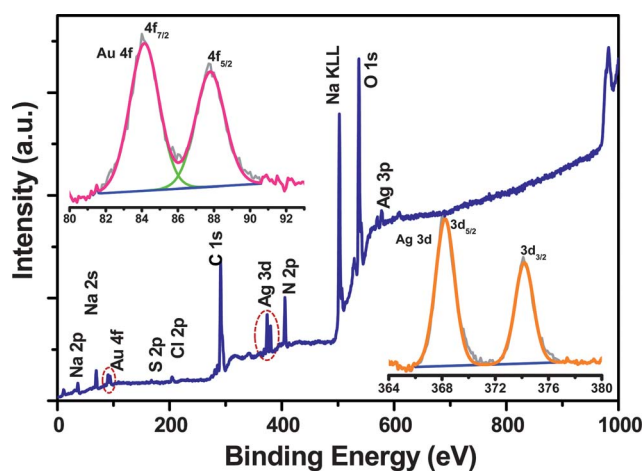
Fig. 4 XPS survey spectrum of AuAg$_{QC}$@BSA showing the presence of metallic Ag and Au (dotted pink circles). Inset: expanded and fitted spectral regions of Au 4f (magenta line) and Ag 3d (orange line).

since they are highly reactive) in view of the large affinity of S to noble metals. The atomic Au : S and Ag : S ratios suggested one cluster per intact protein with excess thiol–thiolate groups. The other possibility for excess sulfur may be free protein molecules. In the SEM-EDAX analysis, the atomic S : Au : Ag ratio was 2 : 1 : 1. The excess content of sulfur can be attributed to the available 34 cysteine residues per protein, which is higher than the required (SR$_{24}$ for (AuAg)$_{38}$) to stabilize the cluster in one
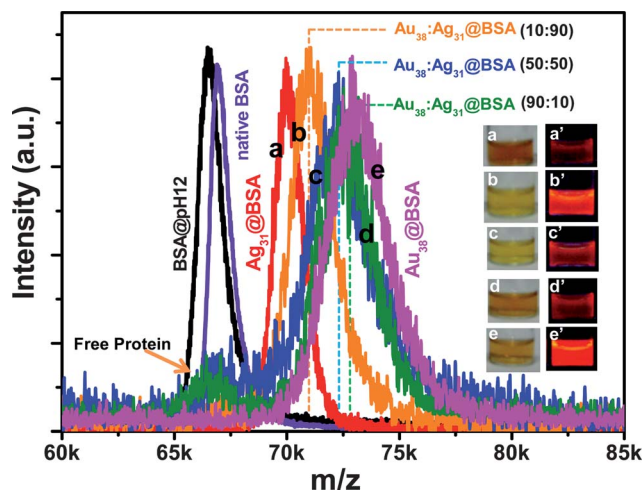
Fig. 5 MALDI MS data shows the tunability of the composition of the AuAg alloy clusters in protein templates. MS of native BSA (violet) and BSA at pH 12 (black). The products of 900 μL Ag$_{QC}$@BSA + 100 μL Au$_{QC}$@BSA (90 : 10) peak at m/z 71 100 (orange trace), 500 μL Ag$_{QC}$@BSA + 500 μL Au$_{QC}$@BSA (50 : 50) peak at m/z 72 300 (blue trace) and 100 μL Ag$_{QC}$@BSA + 900 μL Au$_{QC}$@BSA (10 : 90) peak at m/z 72 800 (olive trace) lie between Ag$_{QC}$ (red trace) and Au$_{QC}$@BSA (magenta trace), suggesting compositional variation in the alloys. Inset photographs: (a) Ag$_{QC}$@BSA, (b) Au$_{QC}$: Ag$_{QC}$@BSA (10 : 90), (c) 50 : 50 Au$_{QC}$: Ag$_{QC}$, (d) Au$_{QC}$: Ag$_{QC}$ (90 : 10) and (e) Au$_{QC}$@BSA under visible light (left) and UV light (right). The ratio mentioned here is v/v, which can also be considered as a molar ratio since Au and Ag solutions of the same molarity were used.

protein, since they may not all participate in the stabilization process. Another sulfur-containing amino acid, the less reactive methionine (~5 per BSA molecule) is also present. All the other elements in the XPS survey spectrum are due to the protein. The presence of Na and Cl is due to the by-products derived from the reagents (Fig. 4).

As AuAg alloys are possible across the entire compositional window, we tried to create clusters of varying composition by mixing appropriate amounts of the as-prepared clusters. The mass spectra of the mixture of clusters (Fig. 5) showed well defined compositions with complete tunability, suggesting the formation of $Au_{1-x}Ag_x$ clusters across the entire compositional window. No parent clusters are seen in the mass spectra. All these clusters are luminescent and the photophysical properties of the alloy clusters formed from the interactions of different ratios of Au_{QC} and Ag_{QC} are currently under investigation. The final composition in the product need not be the same as in the starting materials. The emergence of free protein may indicate that inter-protein metal ion transfer facilitates alloy formation.

### 3. 2. Alloy cluster through galvanic exchange

In another approach, we have synthesized the alloy clusters through galvanic exchange reactions. While the Au and Ag clusters react, a similar reactivity is possible between the cluster core and the Au ions, especially when a galvanic reaction is facile. Reduction of Au^{3+} by an Ag cluster is a possible way to form

alloy clusters, as we have shown before.[12] To test this hypothesis with protein-protected clusters, we added varying amounts of Au^{3+} to the Ag cluster. The mass spectra showed a systematic shift in which the composition of the core continuously altered (Fig. 6A). The initial measurements around one hour showed a mass shift for all the different volumes of 100 mM Au^{3+} added, although the observed mass shift may not represent the alloy cluster formed, since XPS only showed the Au^0 state after 4 h. Hence, we carried out time dependent MS studies for the volume of 25 μL Au^{3+} added to $Ag_{QC}@BSA$. These changes, although observed immediately after mixing, continued for a longer timescale as shown in Fig. 6B. Such clusters are also luminescent, as shown in the ESI (Fig. S3†) and the existence of the alloy was confirmed by EDAX (Fig. S4†). The galvanic nature of this reaction is shown from the formation of AgCl crystallites with well defined morphology in the SEM and EDAX images (Fig. S5†).[12] Note that Cl^- is in solution. In agreement with this, systematic changes in the valence state of gold are seen in the XPS data. While Au^{3+} is taken up as Au^{1+} due to the interaction of the protein, it gradually transforms to Au^0 as time progresses. The Au $4f_{7/2}$ at 85.6 eV due to Au^{1+} decreases in intensity and a peak at 84.0 eV due to Au^0 evolves gradually (Fig. 6D). There is no drastic change seen in the Ag 3d region, as Ag^0 and Ag^+ are similar in binding energy (Fig. 6 D).

There have been a number of reports of reactions of quantum dots, especially reactions such as cation/anion exchange. These exchange reactions are also facile in nanowires, especially in
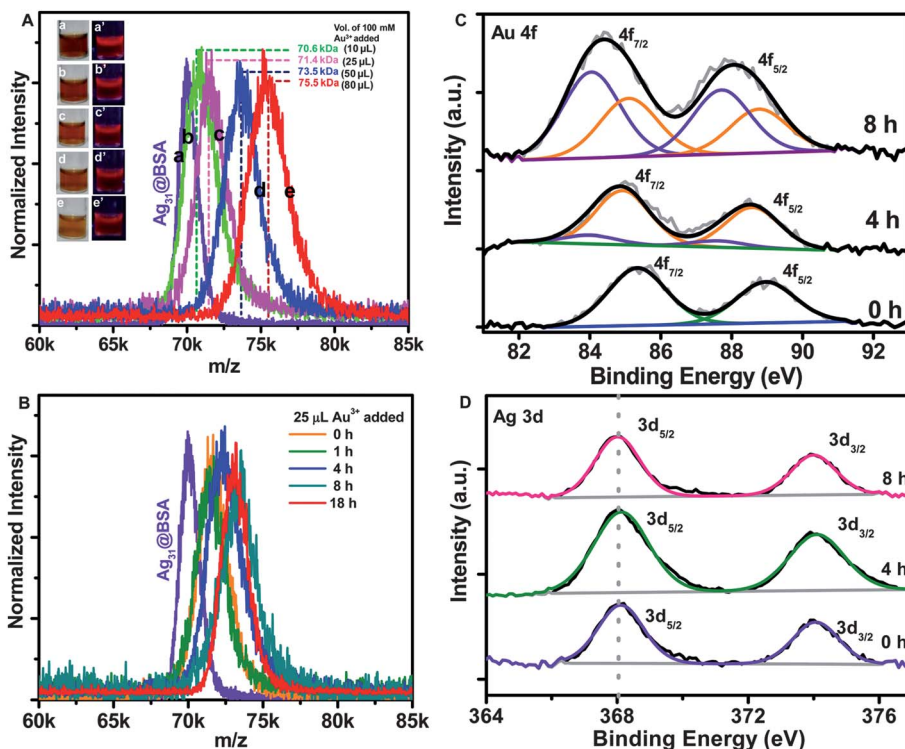
Fig. 6 (A) MALDI MS data of (a) $Ag_{QC}@BSA$ (violet trace), reaction products obtained around one hour after the addition of different volumes of $HAuCl_4$: (b) 10 μL (green trace), (c) 25 μL (magenta trace), (d) 50 μL (blue) and (e) 80 μL (red trace) of Au^{3+}. Inset photographs: the reaction products of $Ag_{QC}@BSA$ with different volumes of Au^{3+} under visible (a–e) and UV (a′–e′) light. (B) Time-dependent MALDI MS data of $Ag_{QC}@BSA$ interacting with Au^{3+} ions to form $AuAg_{QC}@BSA$. Time-dependent XPS spectra of (C) the Au 4f region showing the emergence of zero-valent state and (D) the Ag 3d region.
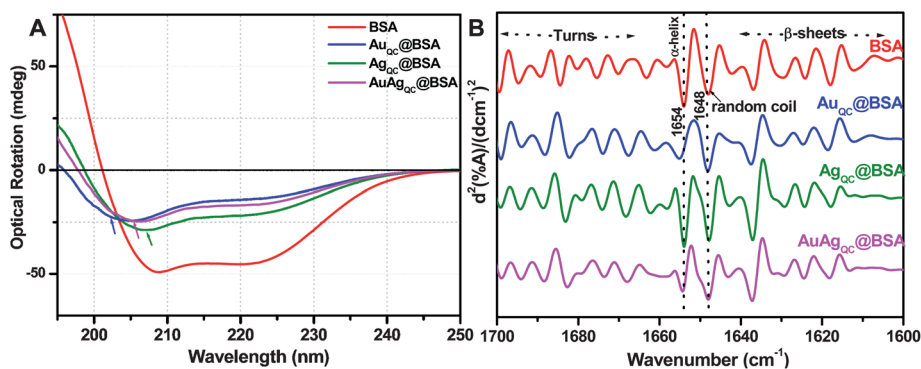
Fig. 7 (A) CD spectra of BSA (red), Ag_{QC}@BSA (green), Au_{QC}@BSA (blue) and $AuAg_{QC}$@BSA (magenta). (B) Second derivative FTIR spectra of amide I region of BSA (red), Au_{QC}@BSA (blue), Ag_{QC}@BSA (green) and $AuAg_{QC}$@BSA (magenta).

shape-conserving transformations.[29,30] Compositional changes leading to core/shell systems are also reported in the literature. Thus, the creation of alloy clusters in protein templates is not surprising. However, the nearly identical nuclearity across the entire compositional window is unprecedented. We assume that it is observed due to the intact protein structure with specific locations of the binding residues. Possibly such restrictions preserve a given cluster's nucleus.

3.3. Conformational changes in the protein

Such metal atom substitution reactions may lead to changes in the protein conformation. These are reflected in the CD spectra where the alloy cluster-containing protein solution exhibits intermediate peaks in comparison to the parent clusters. The calculated data showed the alpha helix content to be 64.5%, 13.8%, 16.5% and 20.7% for BSA, Au_{QC}@BSA, $AuAg_{QC}$@BSA and Ag_{QC}@BSA, respectively (Fig. 7A). The formation of the three different clusters showed a significant loss of alpha helix content. While Ag_{QC} showed minimum and Au_{QC} showed maximum losses, $AuAg_{QC}$ showed an intermediate loss. These results are also supported by vibrational spectroscopic studies, especially IR studies. FTIR has been one of the widely used techniques to probe the changes of the protein's secondary structure. The shifting of bands to higher frequency and the broadening of the bands are the features seen in general. The FTIR spectra showed the expected bands for the protein such as amide I, amide II, amide III and amide A, in the 1600–1690, 1480–1575, 1229–1301 and ~3300 cm^{-1} regions, respectively[15,31,32] (Fig. S6†). The IR second derivative spectra, which are more sensitive to changes, showed that the alpha helix content (indicated by the peak at 1654 cm^{-1}) of the protein decreased to a greater extent in Au_{QC}@BSA and to a lesser extent for Ag_{QC}@BSA. For $AuAg_{QC}$@BSA, the changes were intermediate between the former two (Fig. 7B). These results were corroborated by the CD data, which also suggests that the changes in the structure of the protein observed in $AuAg_{QC}$@BSA are intermediate to those of Au_{QC}@BSA and Ag_{QC}@BSA. These are related to the intermediate conformational changes occurring in the protein molecules due to the alloy cluster.

4. Conclusion

We have demonstrated the synthesis of AuAg alloy quantum clusters with tuneable compositions in a BSA template starting from Au and Ag clusters. MALDI MS suggested the presence of the alloy cluster in BSA. XPS analysis revealed the presence of both Au and Ag in the alloy cluster in the zero-valent state. The rapid interaction between the parent QCs@proteins and the evolution of the compositionally isotropic alloy clusters with a complete absence of the parent clusters is unusual. Inter-protein metal ion transfer leading to the formation of the new hybrid cluster and the concomitant emergence of free protein is apparent from this study. While many questions remain unanswered regarding clusters in proteins, the creation of new materials in the macromolecule template is evident. A complete understanding of protein-protected cluster systems would require several additional experiments like high resolution MS of electrophoretically/chromatographically separated entities and in particular, X-ray crystallography of intact QC@proteins. Efforts are being made in this direction. Such alloy systems with their luminescence and tuneable composition would have interesting applications in the field of catalysis, electronics and medicine. The synthesis of other alloy systems following a similar method using various proteins and metals is likely and the topic is being explored currently.

References

1 R. Jin, *Nanoscale*, 2010, **2**, 343–362 and the references cited therein.
2 M. A. H. Muhammed and T. Pradeep, in *Advanced Fluorescence Reporters in Chemistry and Biology II*, ed. A. P. Demchenko, Springer, Berlin, Heidelberg, 2010, pp. 333–353.
3 P. L. Xavier, K. Chaudhari, A. Baksi and T. Pradeep, *Nano Rev.*, 2012, **3**, 14767, DOI: 10.3402/nano.v3i0.14767 and the references cited therein.
4 L. Shang, S. Dong and G. U. Nienhaus, *Nano Today*, 2011, **6**, 401.

5 J. Zheng, P. R. Nicovich and R. M. Dickson, *Annu. Rev. Phys. Chem.*, 2007, **58**, 409–431.
6 K. M. Harkness, D. E. Cliffel and J. A. McLean, *Analyst*, 2010, **135**, 868–874.
7 T. U. B. Rao, B. Nataraju and T. Pradeep, *J. Am. Chem. Soc.*, 2010, **132**, 16304–16307.
8 C. Kumara and A. Dass, *Nanoscale*, 2011, **3**, 3064–3067.
9 C. Kumara and A. Dass, *Nanoscale*, 2012, DOI: 10.1039/c2nr11781a.
10 Y. Negishi, K. Igarashi, K. Munakata, W. Ohgake and K. Nobusada, *Chem. Commun.*, 2012, **48**, 660–662.
11 A. Murugadoss, N. Kai and H. Sakurai, *Nanoscale*, 2012, **4**, 1280–1282.
12 T. Udayabhaskararao, Y. Sun, N. Goswami, S. K. Pal, K. Balasubramanian and T. Pradeep, *Angew. Chem., Int. Ed.*, 2012, **51**, 2155–2159.
13 J. Xie, Y. Zheng and J. Y. Ying, *J. Am. Chem. Soc.*, 2009, **131**, 888–889.
14 M. A. H. Muhammed, P. K. Verma, S. K. Pal, A. Retnakumari, M. Koyakutty, S. Nair and T. Pradeep, *Chem.–Eur. J.*, 2010, **16**, 10103–10112.
15 P. L. Xavier, K. Chaudhari, P. K. Verma, S. K. Pal and T. Pradeep, *Nanoscale*, 2010, **2**, 2769–2776.
16 A. Mathew, P. R. Sajanlal and T. Pradeep, *J. Mater. Chem.*, 2011, **21**, 11205–11212.
17 Y. Yue, T. Y. Liu, H. W. Li, Z. Liu and Y. Wu, *Nanoscale*, 2012, **4**, 2251–2254.
18 A. Retnakumari, S. Setua, D. Menon, P. Ravindran, M. A. H. Muhammed, T. Pradeep, S. Nair and M. Koyakutty, *Nanotechnology*, 2010, **21**, 055103–12.
19 X. L. Guével, N. Daum and M. Schneider, *Nanotechnology*, 2011, **22**, 275103.
20 S. S. Narayanan and S. K. Pal, *J. Phys. Chem. C*, 2008, **112**, 4874.
21 C. L. Liu, H. T. Wu, Y. H. Hsiao, C. W. Lai, C. W. Shih, Y. K. Peng, K. C. Tang, H. W. Chang, Y. C. Chien, J. K. Hsiao, J. T. Cheng and P. T. Chou, *Angew. Chem., Int. Ed.*, 2011, **50**, 7056–7060.
22 H. Liu, X. Zhang, X. Wu, L. Jiang, C. Burda and J. J. Zhu, *Chem. Commun.*, 2011, **47**, 4237–4239.
23 K. Chaudhari, P. L. Xavier and T. Pradeep, *ACS Nano*, 2011, **5**, 8816–8827.
24 Y. H. Chen, J. T. Yang and K. H. Chau, *Biochemistry*, 1974, **13**, 3350–3359.
25 P. Ramasamy, S. Guha, E. Shibu, T. S. Sreeprasad, S. Bag, A. Banerjee and T. Pradeep, *J. Mater. Chem.*, 2009, **19**, 8456–8462.
26 H. Wei, Z. Wang, J. Zhang, S. House, Y. G. Gao, L. Yang, H. Robinson, L. H. Tan, H. Xing, C. Hou, I. M. Robertson, J. M. Zuo and Y. Lu, *Nat. Nanotechnol.*, 2011, **6**, 93–97.
27 D. Thompson, J. P. Hermes, A. J. Quinn and M. Mayor, *ACS Nano*, 2012, **6**, 3007.
28 G. J. Ashwell, B. U. Wojcik and L. J. Phillips, *Angew. Chem., Int. Ed.*, 2010, **49**, 3508–3512.
29 A. K. Samal and T. Pradeep, *Nanoscale*, 2011, **3**, 4840–4847.
30 X. Guo, Q. Zhang, Y. Sun, Q. Zhao and J. Yang, *ACS Nano*, 2012, **6**, 1165–1175.
31 L. Shang, Y. Wang, J. Jiang and S. Dong, *Langmuir*, 2007, **23**, 2714–2721.
32 A. Dong, P. Huang and W. S. Caughey, *Biochemistry*, 1990, **29**, 3303–3308.